Research Article

25-Hydroxyvitamin D₃-Loaded PLA Microspheres: *In Vitro* Characterization and Application in Diabetic Periodontitis Models

Hao Li,[1] Qi Wang,[1] Yu Xiao,[1] Chongyun Bao,[1] and Wei Li[1,2]

Abstract. This study aimed at the preparation of a sustained-release 25-hydroxyvitamin D₃ (25OHD) treatment for diabetic periodontitis, a known complication of diabetes. 25OHD-loaded polylactic acid (PLA) microspheres were prepared using oil-in-water emulsion–solvent evaporation method. The prepared microspheres exhibited intact surfaces, with average sizes ranging from 42.3 to 119.4 μm. The encapsulation efficiency ranged from 79.2% (*w/w*) to 88.5% (*w/w*), and the drug content was between 15.8% (*w/w*) and 17.8% (*w/w*). Drug release from the produced microspheres followed a near-to-zero-order release pattern and lasted over 10 weeks. In an *in vitro* model of diabetic periodontitis, the abnormal morphological changes and the decrease in the cell viability of bone marrow stromal cells could be effectively attenuated after the 25OHD-loaded microsphere application. Additionally, in a rat model of diabetic periodontitis, alveolar bone loss was inhibited and osteoid formation in the periodontium was promoted upon 25OHD-loaded microsphere treatment. In conclusion, 25OHD-loaded PLA microspheres may provide an effective approach for the treatment of this disease.

KEY WORDS: 25-hydroxyvitamin D₃; bone marrow stromal cell; diabetic periodontitis; microsphere.

INTRODUCTION

Diabetes is one of the main threats to human health in the twenty-first century. It is a heterogeneous group of metabolic disorders that are characterized by hyperglycemia (1). Both forms of diabetes, type 1 and type 2, can promote the development of periodontal disease and aggravate the severity of periodontal infections. Periodontitis superimposed on diabetes, also known as diabetic periodontitis, often causes great damage to the alveolar bone, eventually leading to tooth loss. This disease has been considered as an important complication of diabetes (2).

It is believed that bone loss in diabetic periodontitis is strongly associated with the reduction of osteogenic cells. Bone marrow stromal cells (BMSCs) are one of the key cells that have the potential to differentiate to osteogenic cells in the periodontium. Their impaired activity and abnormal death can result in decreased bone formation (3). Both bacterial toxin and high blood glucose cause detrimental effects on bone-forming cells and their progenitors, including BMSCs, and promote alveolar bone resorption (1,4–6).

It has been reported that both periodontal pathogens and hyperglycemia are crucial in the etiology of diabetic periodontitis (7). The Gram-negative bacterium *Actinobacillus*

actinomycetemcomitans is considered as a major causative agent of common forms of human periodontitis. It produces different toxins to cause periodontal destruction, and its co-culture with periodontal tissue cells has been chosen for mimicking periodontitis *in vitro* (8,9). A high-glucose medium has been accepted to reflect hyperglycemia in experimental diabetes research. The periodontal cells cultivated in this type of medium are widely used for investigating the change of periodontal tissues in diabetes (1,10). In *in vivo* researches, a combination of a high-fat diet and streptozotocin (STZ) injection in rats is often chosen to induce diabetes models (11,12). This model is cost-effective and has the metabolic profile matching this human disease. Ligature placement around molars is used to establish models of periodontitis superimposed on diabetes in many studies (13,14). After tying ligatures, an obvious inflammatory response and tissue destruction in the periodontium can be induced in diabetic rats (13,14).

In recent years, 25-hydroxyvitamin D₃ (25OHD) has been found to be important for the regulation of cell proliferation and death (15,16). Low serum 25OHD concentrations are linked to periodontal destruction in periodontitis as well as osteoporosis in diabetes (17,18). *In vitro* experiments demonstrate the regulatory effect of 25OHD on the viability and proliferation of osteogenic cells and their progenitors, including BMSCs (19). These studies indicate that 25OHD supplementation may impact BMSC viability in the periodontium and subsequently exert beneficial effects on diabetic periodontitis. Bone formation and maturation is generally a long-term process, and the healing of alveolar bone defect often takes over 10 weeks, especially under the condition of diabetes (20,21). Local application of 25OHD may keep the drug concentration and activity in periodontal

---

Hao Li and Qi Wang contributed equally to this work as first authors.

[1] State Key Laboratory of Oral Diseases, West China Hospital of Stomatology, Sichuan University, 14 3rd Section S Renmin Road, Chengdu 610041, China.
[2] To whom correspondence should be addressed. (e-mail: weilee1224@gmail.com; e-mail: leewei2000@sina.com)

tissues and reduce 25OHD degradation before it exerts biological functions in the target area. Thus, the long-period local supplementation of 25OHD in periodontal tissues has great potential in the management of diabetic periodontitis. But currently, there are few reports on the sustained delivery system for 25OHD application.

Many studies indicate that polylactic acid (PLA) formulations containing therapeutic molecules exhibit no untoward reactions, either locally or systemically, when used in therapeutic applications (22). PLA microspheres can effectively deliver therapeutic agents in a sustained-release manner (23). The formulation parameters of PLA microspheres, including particle size and encapsulation efficiency, can also be optimized according to the clinical demand (22). Therefore, PLA microspheres may provide a method for prolonging the therapeutic effect of 25OHD on periodontal tissues.

Several factors have been considered to affect the properties of the produced PLA microspheres, such as PLA concentration, emulsifier polyvinyl alcohol (PVA) concentration, and homogenizer speed in oil-in-water (o/w) emulsion–solvent evaporation method. Their alteration can contribute to changes in particle size, encapsulation efficiency, drug release, etc. In this work, we investigated the preparation of 25OHD-loaded PLA microspheres with optimized characteristics and evaluated the biological effect of this delivery system on both *in vitro* and *in vivo* diabetic periodontitis models.

MATERIALS AND METHODS

Materials

STZ, 25OHD, and 3-(4,5-dimethylthiazol-2-yl)-2,5-diphenyltetrazolium bromide (MTT) were purchased from Sigma-Aldrich, Inc. (St. Louis, MO). PLA (molecular weight, 200,000 Da) and PVA (partially hydrolyzed; degree of hydrolysis, 88%) were from Daigang Biomaterial Co. Ltd. (Jinan, China). Brain heart infusion broth was from Becton Dickinson and Company (Sparks, MD). Alpha-minimum essential medium (α-MEM) was from GibcoBRL (Grand Island, NY).

Preparation of the Microspheres

Microspheres were prepared using o/w emulsion–solvent evaporation method as previously reported (24). Different weights of PLA were dissolved in 5 mL of dichloromethane to make solutions of 4–8% (*w/v*). Amounts of 25OHD were dissolved in the organic phase to make a drug/PLA ratio of 1:4. Then, the organic phase was added to 100 mL aqueous solution of PVA and stirred at 800–1,000 rpm for 3 h. The produced microspheres were collected by centrifugation at 6,000 rpm, washed thrice with distilled water, and lyophilized overnight. Drug-free microspheres were prepared with the same procedure without 25OHD addition.

Characterization of the Microspheres

Morphology of Microspheres

Lyophilized microspheres were examined using a scanning electron microscope (SEM; Jeol JSM-5400 LV, Jeol Ltd., Tokyo, Japan).

Yield of Microspheres

The produced microspheres were collected by centrifugation, lyophilized, and weighed. The yield was calculated as follows (25):

$$\% \text{ Yield} = (\text{Weight of microspheres})/$$
$$(\text{Theoretical weight of microspheres}) \times 100$$

Microsphere Size Analysis

The size distribution of microspheres was investigated using a Mastersizer S laser diffractmeter (Malvern Instruments, Malvern, Worcestershire, UK). The particle size of the microspheres was described as the average diameter. The equivalent volume diameters at 90% (D_{90}), 50% (D_{50}), and 10% (D_{10}) cumulative volumes were examined, respectively, and the mean diameter was taken as the average of the D_{10}, D_{50}, and D_{90} values. Span value was calculated as follows (26):

$$\text{Span} = (D_{90} - D_{10})/D_{50}$$

Drug Content and Encapsulation Efficiency

Amounts of the prepared microspheres were dissolved in 20 mL dichloromethane and 25OHD was analyzed using a UV/Vis spectrophotometer (U-3900H, Hitachi, Chiyodaku, Japan) at 265 nm. Drug-free microspheres were subjected to the same procedure; the resulting solution was used as a blank.

Drug content (in percent *w/w*) and encapsulation efficiency (in percent) were calculated using the following formulae, respectively (27,28):

$$\% \text{ Drug Content} = (\text{Drug in microspheres})/(\text{Mass of microspheres}) \times 100$$

$$\% \text{ Encapsulation Efficiency} = (\text{Actual amount of drug in microspheres})/$$
$$(\text{Theoretical amount of drug in microspheres}) \times 100.$$

Release Study

Ten-milligram 25OHD-loaded microspheres were suspended in 6 mL phosphate-buffered saline (PBS, pH 7.4) in tubes under constant shaking at 60 rpm at 37°C. The release experiments were carried out as previously reported (29). Drug-free microspheres were subjected to the same procedure, and the supernatant was used as the blank at the same time intervals. The drug release test lasted 10 weeks.

Microsphere Degradation Morphology and pH Measurement

Ten-milligram prepared microspheres from formula 3 was placed in 6 mL PBS (pH 7.4) and shaken at 60 rpm at 37°C. At predetermined time intervals, degradation pH values were detected and the PBS containing microspheres were

centrifuged at 3,000 rpm. The residue was collected and investigated using SEM.

25OHD-Loaded Microspheres Applied in an *In Vitro* Diabetic Periodontitis Model

Cell Isolation and Culture

BMSCs were obtained from male Wistar Hanover rats (100–120 g; Experimental Animal Laboratory of Sichuan University) following the *Guidelines for Care and Use of Laboratory Animals in Sichuan University*. The femora and tibiae were dissected from rats and cell isolation and culture in α-MEM with antibiotics was carried out as previously reported (30). All cells were incubated at 37°C under an atmosphere of 5% CO_2. The medium was changed every 3 days and cells were used at passage 3.

In Vitro Diabetic Periodontitis Model and Microsphere Application

One week before the establishment of a diabetic periodontitis-like environment, all media used were changed to those without antibiotics. Afterwards, BMSCs were seeded in six-well plates (10^4 cells/well) and grown under standard cell culture conditions. These cells were divided into different groups as follows: normal control (N); diabetic periodontitis without treatment (DPW); and diabetic periodontitis with different concentrations (1×10^{-2}, 1.5×10^{-2}, 2×10^{-2}, 2.5×10^{-2}, 3×10^{-2}, and 3.5×10^{-2} g/L microspheres in the medium, respectively) of drug-free or 25OHD-loaded microspheres (DPF1, DPF1.5, DPF2, DPF2.5, DPF3, DPF3.5, DPV1, DPV1.5, DPV2, DPV2.5, DPV3, and DPV3.5). *A. actinomycetemcomitans* strain ATCC 29522 was obtained from the State Key Laboratory of Oral Diseases of Sichuan University (Chengdu, China). Addition of *A. actinomycetemcomitans* at a multiplicity of infection (bacteria to cells) of 10:1 in all diabetic periodontitis groups was followed to simulate periodontal infection (31). After incubation with *A. actinomycetemcomitans*, the BMSCs in these groups were washed three times with PBS and cultured in high-glucose medium with 12 mmol/L D-(+)-glucose to mimic the local microenvironment of diabetes (1). Cells in the N group were maintained in the normal standard medium. Then, the media of the groups with drug-free or 25OHD microsphere treatment were supplemented with corresponding microspheres from formula 3 and maintained for 3 days of culture.

Cell Morphology Examination and MTT Assay

After 3 days of culture with microspheres, the BMSCs in all groups were washed with PBS and examined using a digital microscope camera (Leica MZ FLIII, Leica, Wetzlar, Germany). Then, an MTT assay was used to determine the cell viability.

25OHD-Loaded Microsphere Applied in an *In Vivo* Diabetic Periodontitis Model

Experimental Design

Forty male Wistar Hanover rats (160–180 g) were purchased from Dossy Co. (Chengdu, China). Animal treatment was approved by the institutional committee for animal use and care in Sichuan University. All rats were housed at a constant temperature (22°C) with humidity of 45–55% in a 12-h light/dark cycle. They were randomly divided into N, DPW, diabetic periodontitis with drug-free microsphere treatment (DPF), and diabetic periodontitis with 25OHD-loaded microsphere treatment (DPV) groups. There were ten rats in each group.

Diabetic Periodontitis Rat Model and Microsphere Application In Vivo

Control rats were fed low-fat food (12 kcal% fat; Dossy Co.). Rats in the DPW, DPF, and DPV groups were fed high-fat food (58 kcal% fat; Dossy Co.) for 2 weeks and then were fasted for 12 h before a single intraperitoneal injection of STZ (35 mg/kg). Blood from the rat vein tails was collected 1 week after STZ treatment and used to determine the fasting blood glucose. Rats with a fasting blood glucose level above 13.89 mmol/L were considered diabetic (12). After confirmation of diabetes, all rats consumed the low-fat food and periodontitis was induced by tying silk ligatures around both maxillary second molars in the DPW, DPF, and DPV groups (13). Four weeks after ligature placement, ligatures were removed and the periodontal pocket depth of the maxillary second molars was assessed using a periodontal probe. DPF and DPV rats were treated with corresponding microspheres from formula 3. These microspheres were placed into the periodontal pockets at a dose of 1 mg/mm pocket depth.

Fasting Blood Glucose Test

The rat tail veins were pierced with a needle. Blood from the tails was harvested 1 week after STZ treatment and at killing and was used to determine the fasting blood glucose level using a glucometer (OneTouch Glucometer, LifeScan, Milpitas, CA).

Histological Analysis of the Periodontium

All rats were killed 10 weeks after microsphere treatment. Rat maxillae were harvested at killing. Then, they were fixed in 4% paraformaldehyde, decalcified in 10% EDTA, and embedded in paraffin (14). Thin sections (5 μm) were cut and detected using hematoxylin and eosin (H&E) staining. The mid-interproximal region between the first and second maxillary molars was examined in each specimen, and bone loss and areas of osteoid formation were assessed as previously reported (14,32). Both sides of the maxillae were investigated; the averages of these measurements of both sides were calculated to represent the sample.

Statistical Analysis

Data were calculated and shown as the mean±SD. Differences in parameter mean values were analyzed using one-way analysis of variance followed by SNK-q multiple comparisons. Statistical significance was defined as $P<0.05$.

RESULTS AND DISCUSSION

Morphological Characteristics and Microsphere Size

SEM photographs of the prepared 25OHD-loaded microspheres with different formulation parameters were shown in Fig. 1. These microspheres were spherical in shape with intact surfaces.

The characteristics of the drug-loaded PLA microparticles with different formulation parameters, including homogenizer speed, PVA concentration, and PLA concentration, were summarized in Table I. The average size of 25OHD-PLA microspheres decreased as the homogenizer speed increased. The explanation may be that higher homogenizer speeds lead to a more vigorous stirring of PLA particles and provide the force to separate the particles (33). The microsphere mean size became lager as the PVA concentration decreased. This result was in agreement with the literature (33,34). As the PVA concentrations decrease, the surfactants are less likely to form tighter micelles around the PLA microspheres, hence making their size greater. It was also seen in Table I that the average size was increased with elevated PLA concentration. Lower polymer concentrations are considered to make the polymer molecules further apart before synthesis and result in smaller particle sizes (33).

The span value is often chosen to indicate the uniformity of microsphere sizes from different formulae. The higher the span value, the lower the uniformity of the size distribution (35). The span values ranged from 1.03 to 2.28 in this experiment; the microspheres produced at lower homogenizer speeds exhibited increased span values (Table I). It could be explained on the basis that lower homogenizer speeds reduced the shearing action, resulting in larger droplets during the emulsification and, consequently, more microspheres with larger sizes.

Yield, Drug Content, and Encapsulation Efficiency

The yield, drug content, and encapsulation efficiency of the 25OHD-loaded PLA microspheres produced with different formulae were presented in Table I. The production yield ranged from 61.3% to 78.4%. Processing of the drug-loaded PLA microspheres at a higher homogenizer speed provided a lower yield. This might be explained partly by the difficulty in collecting the produced small particles.

It was observed in Table I that the homogenizer speed, PVA concentration, and PLA concentration affected the encapsulation efficiency of the microspheres as well as the drug content. As the homogenizer speed increased, the encapsulation efficiency decreased. It has been reported that drug crystals could be dispersed and suspended in the oil phase (29). As the average microsphere size became smaller, the size range of drug crystals suitable to be encapsulated might become narrower, so lower encapsulation efficiency was observed (29). When the PVA concentration was reduced, the encapsulation efficiency was enhanced, as shown in Table I. This increase in encapsulation efficiency might be associated with the enhanced microsphere size when a lower PVA concentration was employed. It was also seen that the encapsulation efficiency was elevated with increased PLA concentration. The larger microsphere size resulting from higher PLA concentrations may improve the encapsulation efficiency. On the other hand, efficiency elevation may be associated with the enhanced amount of the added 25OHD, to make the drug/PLA ratio constant.

In Vitro Drug Release

25OHD release from the PLA microspheres followed a near-to-zero-order release pattern. The process of drug release lasted over 10 weeks (Fig. 2). It is known that the degradation of the PLA microparticles includes water penetration into the microsphere matrix and the following bulk erosion. As the erosion progresses, the matrix porosity increases and the encapsulated drug release by diffusion occurs
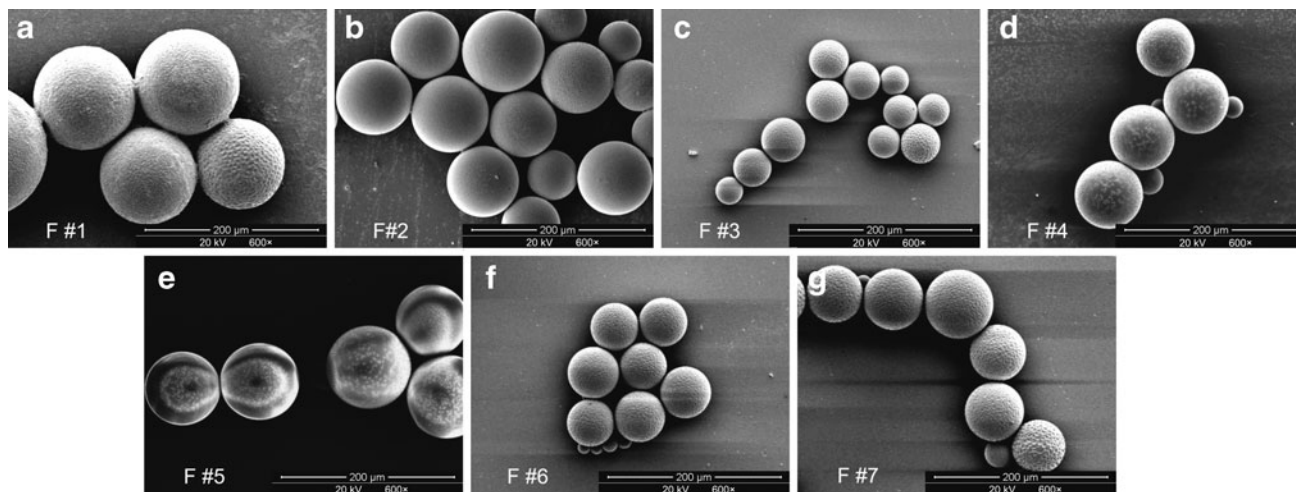

Fig. 1. Images of microspheres obtained using scanning electron microscopy. **a–g** Microparticles from formulae 1–7, respectively

Table I. Formulation Parameters and Properties of 25OHD-Loaded PLA Microspheres from Different Formulae

Formula no.	Homogenizer speed (rpm)	PVA conc. (%, *w/v*)	PLA conc. (%, *w/v*)	Yield (%, *w/w*)	Average diameter (μm)	Span value	Drug content (%) (*w/w*±SD)	Encapsulation efficiency (%) (*w/w*±SD)
1	800	0.4	4	78.4±0.9	119.4±10.2	1.28±0.03	17.3±0.2	86.7±1.4
2	900	0.4	4	66.1±1.4	85.8±7.5	1.21±0.04	16.9±0.2	84.5±1.0
3	1,000	0.4	4	62.7±0.8	42.3±5.8	1.10±0.02	15.8±0.5	79.2±1.9
4	1,000	0.3	4	68.2±0.6	73.6±8.1	1.06±0.05	16.7±0.3	83.3±1.5
5	1,000	0.2	4	65.0±1.2	89.2±6.7	1.03±0.08	17.2±0.5	85.9±2.4
6	1,000	0.4	6	61.3±0.5	50.7±7.4	1.15±0.04	17.1±0.3	85.2±1.6
7	1,000	0.4	8	64.6±1.3	64.2±5.2	1.16±0.05	17.8±0.2	88.5±1.1

Data represent the mean±SD (*n*=3). Yield: *P*<0.01 (1:2); *P*<0.05 (2:3). Average diameter: *P*<0.01 (1:2, 2:3, 3:4, 4:5); *P*<0.05 (3:6, 6:7). Span value: *P*<0.05 (1:2, 2:3). Drug content: *P*<0.05 (1:3, 2:3, 3:4, 3:5, 3:6, 6:7). Encapsulation efficiency: *P*<0.05 (1:2, 2:3, 3:4, 4:5, 3:6, 6:7)
PVA polyvinyl alcohol, *PLA* polylactic acid

(36). Drugs can be slowly released with gradual degradation of the PLA microspheres. The initial burst drug release was largely due to the 25OHD located on the surface layer.

The release properties of the produced microspheres were optimized with the adjusted formulation parameters. It was seen in Fig. 2 that the microparticles prepared at higher stirring speeds had greater drug release in the initial burst period. It might be attributed to the increase in specific surface area with the decrease in microsphere size. However, a lower speed increases the drug content, and increasing drug release causes more pores in the microsphere matrix, resulting in an enhanced degradation and release rate. Hence, the microspheres prepared at a lower homogenizer speed exhibited faster 25OHD release after the initial burst period and a more cumulative release at the end of the experiment. But the path for the drug diffusion to the external phase increases with greater microsphere size (29), contributing to delayed drug diffusion. This effect might outweigh the rapid release resulting from the elevated drug content, so 25OHD release remained slow during the degradation of microspheres from formula 1. As shown in Fig. 2, the PVA concentration also influenced the release pattern. When lower PVA concentrations are used, the microsphere size becomes lager, resulting in longer drug diffusion paths and an initially slow 25OHD release. However, a reduced PVA concentration can improve drug content, leading to the increase in degradation and release rate (29). Therefore, the microspheres produced at lower PVA concentrations showed increasing drug release after the initial burst period and a more cumulative release in the subsequent period. Furthermore, PLA concentration was another factor that could alter the release pattern (Fig. 2).

Hindered 25OHD release could be seen with enhanced polymer concentration. Other researchers have found that the microsphere matrix becomes denser when higher polymer concentrations are used (36). Drug migration to the microsphere surface can be slowed down with the increase in matrix density.

It is believed that the increase in polymer molecular weight often decreases microsphere degradation and, therefore, drug release rate (37). However, in this study, some microspheres of high-molecular-weight PLA exhibited a relatively short degradation duration and released almost all of the encapsulated 25OHD in 10 weeks. The explanation could be as follows: These microspheres were fabricated at a relatively high PVA concentration. Some residual PVA might exist in the microspheres, leading to the decreased crystallinity of PLA and the enhanced hydrophilicity of microspheres, therefore accelerating the degradation. Additionally, these microspheres had many pores and channels left by evaporation in the matrix, which could increase the drug diffusion and microsphere degradation. Furthermore, the small-sized microspheres had lager specific surface areas, which also promoted degradation and drug release.

Microsphere Degradation and pH Measurement

The degradation of drug-loaded PLA microspheres was assessed using SEM (Fig. 3). The initial morphological change was the increased surface roughness. The microsphere surface was much rougher with more fossea and pores after 28-day degradation. The microspheres exhibited a marked surface
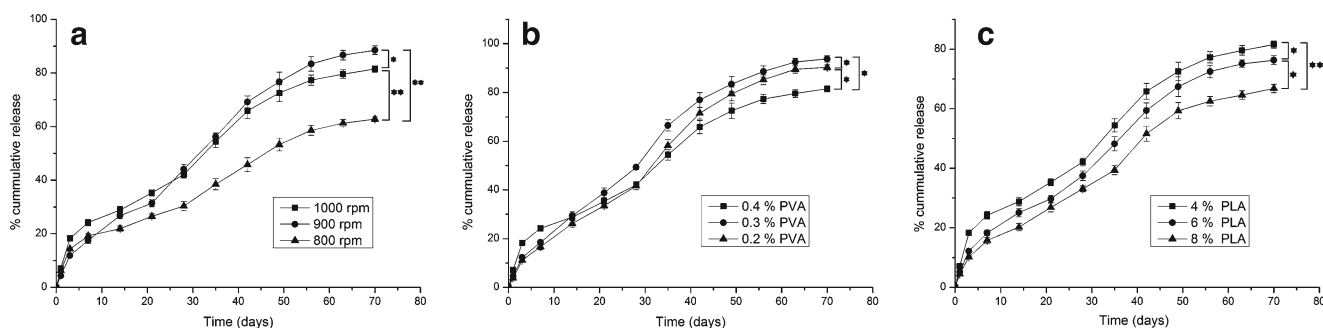

Fig. 2. Effect of different formulation parameters on 25OHD release from microspheres. **a** Homogenizer speed. **b** PVA concentration. **c** PLA concentration. Data represent the mean±SD (*n*=3). **P<0.05; ***P<0.01 for the cumulative release at the end of the release test
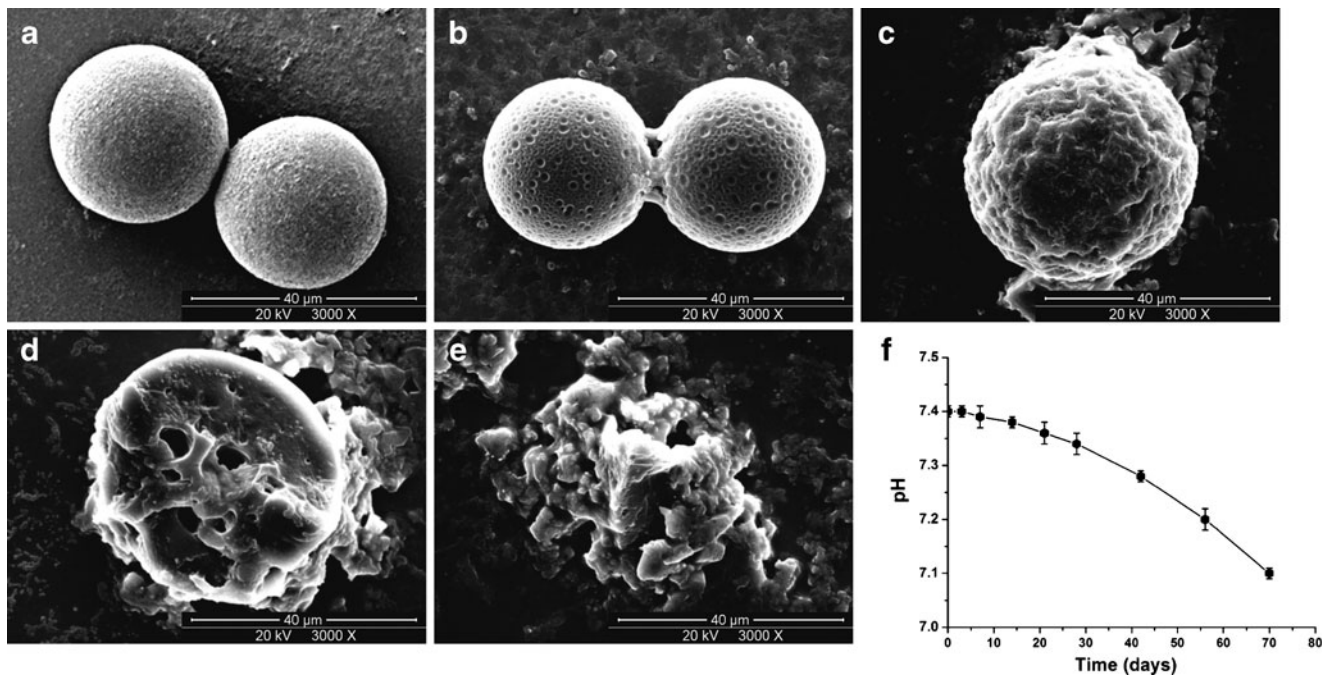
Fig. 3. 25OHD-loaded microspheres produced at 0.4% PVA (*w/v*), 4% PLA (*w/v*), and 1,000 rpm (formula 3) were incubated in PBS (pH 7.4) at 37°C; images of degradation were obtained using scanning electron microscopy. **a–e** Microspheres after incubation for 0, 7, 28, 56, and 70 days, respectively. **f** Degradation medium pH

erosion and pitting after 56-day incubation, and some of them lost their spherical shapes. On the 70th day, the microspheres were obviously crumpled and collapsed. Additionally, the profile of pH changes in the degradation medium (Fig. 3) showed that the medium pH began to drop slightly after 14 days. A more obvious pH decrease started after 28 days. At the end of the degradation experiment, the medium pH dropped by approximately 0.3.

The degradation of PLA has been described by hydration, followed by ester bond hydrolysis, and subsequent molecular weight decrease and microspherical weight loss (38). It takes time for water to permeate into the matrix, so the cleavage of the polymer chains inside the matrix bulk by hydrolysis or large amounts of production of acidic shorter-chain moieties do not occur in the early stage. The acidic products are entrapped within the polymer bulk in this stage, so the pH decrease of the degradation medium is not obvious. As the oligomer fraction continues to form and becomes soluble in the aqueous medium, more polymer chains cleave and more trapped acidic fractions migrate to the external aqueous phase, resulting in the noticeable decrease in medium pH (36).

Effects of the Produced Microspheres on the *In Vitro* Diabetic Periodontitis Model

Periodontal lesions caused by periodontitis are usually small-sized, leaving limited space for the drug-loaded material application in the treatment. The microspheres from formula 3 had the smallest average diameter and were more suitable for clinical application, so they were chosen in the experiment on the diabetic periodontitis model. High glucose and *A. actinomycetemcomitans* have been found to be crucial in the onset and development of diabetic periodontitis (7). Periodontal cells cultivated in high-

glucose medium are widely used for studying the periodontal lesion under the condition of diabetes (1,10); these cells, co-cultured with *A. actinomycetemcomitans*, have also been accepted for establishing periodontitis models *in vitro* (8,9). Thus, BMSCs cultured with *A. actinomycetemcomitans* in the high-glucose medium were chosen to establish an *in vitro* diabetic periodontitis model.

As shown in Fig. 4, infection with *A. actinomycetemcomitans* in the high-glucose medium caused morphological alterations of the BMSCs, such as cell shrinkage and detachment. These changes were obvious, with a marked decrease in cell number and increase in apoptotic fractions in the DPW group and the groups with drug-free microsphere treatment. A significant reduction in cell viability was also seen in these groups in the MTT test compared with the N group. The results indicated the negative effect of this diabetic periodontitis-like environment on BMSCs. These findings were also consistent with other reports on the effect of bacterial infection or hyperglycemia on periodontal cells (6,8,39).

The morphology and viability of the *A. actinomycetemcomitans*-infected BMSCs in the diabetic-like environment were influenced by 25OHD-loaded microspheres (Fig. 4). As the concentration of 25OHD-loaded microspheres was enhanced from 1×10^{-2} to 2.5×10^{-2} g/L in the medium, abnormal cell changes caused by the diabetic periodontitis-like environment were attenuated. There was no significant difference in cell viability among the DPW, DPV1, and DPV1.5 groups. When this *in vitro* model of diabetic periodontitis was treated with 2.5×10^{-2} g/L 25OHD-loaded microspheres, high cell viability was observed. Meanwhile, cell shrinkage and structure destruction were greatly improved in the DPV2.5 group. Research on peritoneal mesothelial cells demonstrates that activated 25OHD can reverse the inhibition of cell viability
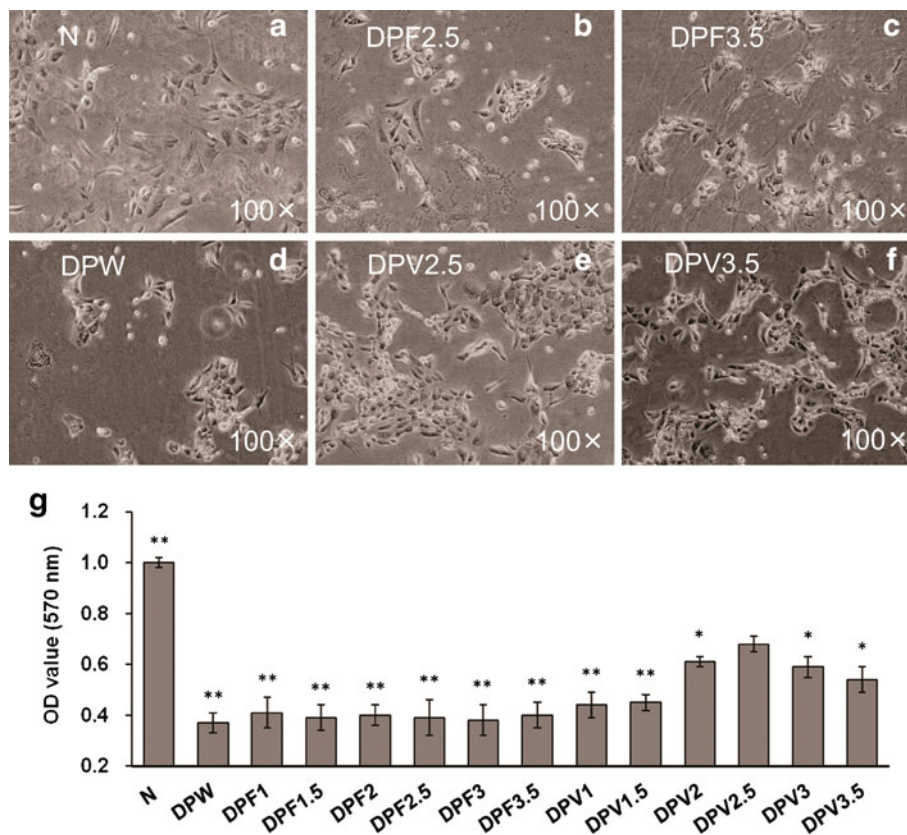
Fig. 4. MTT assay showing the cell viability of BMSCs cultivated with different concentrations of drug-free microspheres or 25OHD-loaded microspheres. Data represent the mean±SD (n=3). *$P<$ 0.05; ** $P<0.01$ *vs.* the DPV2.5 group **g**. There was no significant difference among the groups with different concentrations of drug-free microspheres and no significant difference between the DPW group and any group with drug-free microspheres. Photographs represent the BMSCs of the N group **a**, DPF2.5 group **b**, DPF3.5 group **c**, DPW group **d**, DPV2.5 group **e**, and DPV3.5 group **f**

and the increase in cell apoptosis by high glucose plus the main toxin of *A. actinomycetemcomitans* (40). Other studies have also shown that 25OHD inhibits abnormal cell death caused by oxidative stress and other apoptosis stimulations, which can result from hyperglycemia or infection (41,42). These findings suggest that 25OHD microspheres may improve diabetic periodontitis through protecting BMSCs against demise caused by infection and high glucose. The results of this work further demonstrated that 25OHD could exert a protective function on BMSCs only when the drug released from microspheres reached certain concentrations. The therapeutic effect of sustained 25OHD supplementation could be obtained through changing the initial amount of 25OHD-loaded microspheres.

When the concentration of the drug-loaded microsphere was enhanced to 3×10^{-2} and 3.5×10^{-2} g/L, however, the beneficial effect of these microparticles was weakened. More cell apoptotic fractions and decreasing viability were found in the DPV3 and DPV3.5 groups compared with the DPV2.5 group (Fig. 4). These observations indicated that an overdose of 25OHD had detrimental impacts on BMSCs, as previously reported (19). Thus, the amount of 25OHD-loaded microspheres should be further adjusted in clinical applications.

Effects of the Produced Microspheres on the *In Vivo* Diabetic Periodontitis Model

Fasting Blood Glucose of the Rats with Diabetic Periodontitis

The fasting blood glucose levels of all rats were measured and shown in Fig. 5. One week after STZ injection, the DPW, DPF, and DPV groups exhibited hyperglycemia (fasting blood glucose level above 13.89 mmol/L) after a 10-h fast compared to the N group, demonstrating that the diabetic model was established. The DPW, DPF, and DPV groups had significantly higher fasting blood glucose levels than the N group at killing, and there was no considerable difference among the three diabetic groups. There have been reports that systemic supplementation of vitamin D improves glycemic control in diabetic animals and attenuates diabetes in humans (43,44). However, the data in this experiment showed no effect of local 25OHD-loaded microsphere application on the glycemic level in diabetic rats. The possible explanation could be that 25OHD released from the microsphere was mainly located and metabolized in the periodontium and could not result in the effective serum concentration to influence the blood glucose.
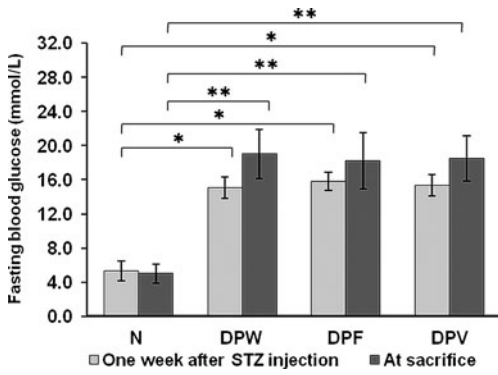
Fig. 5. Fasting blood glucose levels of N, DPW, DPF, and DPV rats measured 1 week after STZ treatment and at killing. Data are presented as the mean±SD ($n=10$). *$P<0.05$; **$P<0.01$

Effects of the Produced Microspheres on the Alveolar Bone

As shown in Fig. 6, bone loss was induced in all rats with diabetic periodontitis, as evidenced by an increase in the distance from the cemento-enamel junction to the highest peak of the interproximal bone. According to previous reports, placement of ligatures around animal molars facilitates bacterial invasion of the periodontium, so it has been accepted to induce periodontitis in both diabetic and non-diabetic rats (14,45). In this experiment, bone loss was dramatically

decreased in DPV rats compared to diabetic periodontitis rats without 25OHD-loaded microsphere treatment (DPW and DPF rats), while it did not significantly differ between DPW and DPF rats (Fig. 6). This observation may be attributed to the sustained release of 25OHD from the microspheres. As the stable metabolite of vitamin D in the body, 25OHD regulates the viability and proliferation of osteogenic progenitors and subsequently affects the maintenance of bone mass (19). Metabolites of vitamin D can be inactivated by various tissue cells, so vitamin D supplementation is often of long period in the management of chronic diseases (46,47). Current clinical trials have shown the improvement of periodontitis by long-term oral vitamin D supplementation (48,49). Our previous study has also demonstrated the amelioration of alveolar bone loss in diabetic periodontitis with 8-week intraperitoneal supplementation of 25OHD (43).

Bone formation is usually coupled with bone resorption and limits net bone loss under the condition of periodontal inflammation. The area of osteoid is an important bone formation-related parameter and often chosen to assess the protective effect of drugs on bone loss. As shown in Fig. 6, the amount of osteoid formation was lower in the three groups with diabetic periodontitis than in the normal group, but it was higher in DPV rats compared to DPW or DPF rats. Our results indicated the promotion of periodontal bone regeneration by 25OHD-loaded microspheres in diabetic periodontitis. There has been evidence that vitamin D metabolites not only inhibit
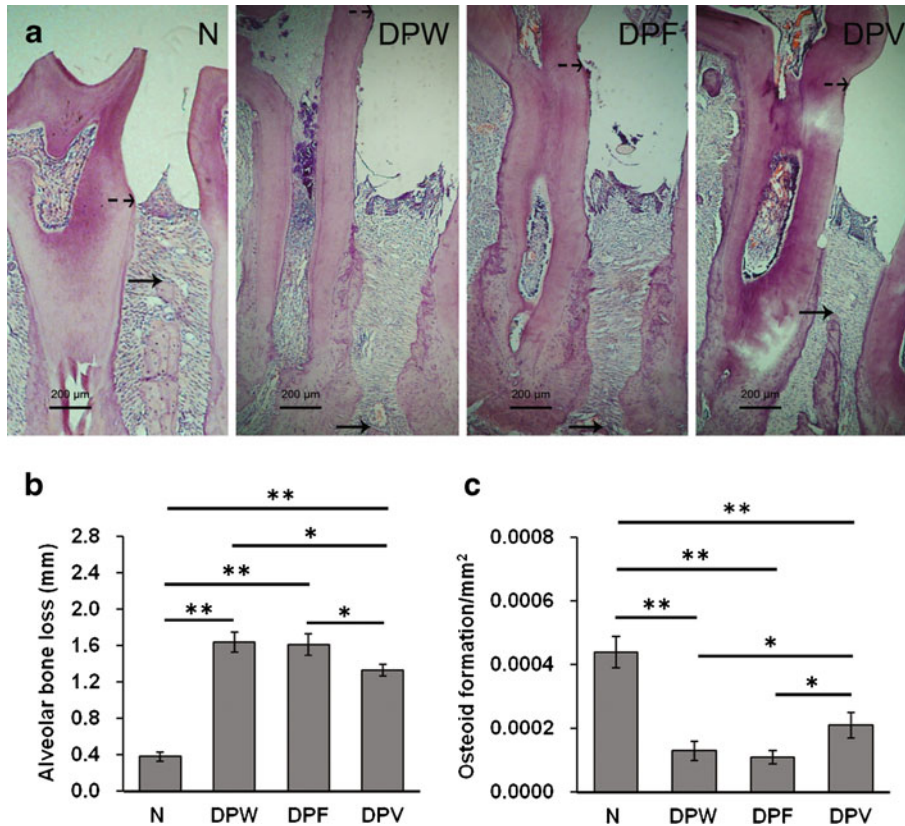

Fig. 6. Mid-interproximal region between the first and second maxillary molars examined in each rat specimen. Bone loss was determined as the distance between the cemento-enamel junction (*dotted arrow*) and the highest peak of the interproximal bone (*solid arrow*) **a**. Alveolar bone loss **b** and the area of osteoid formation **c** were measured in H&E-stained sections. *$P<0.05$; **$P<0.01$. Data represent the mean±SD ($n=10$)

the apoptosis of osteogenic progenitors under the high-glucose condition but also promote bone-forming cell differentiation, contributing to more bone formation (19). In this study, there was no significant difference of the area between DPW and DPF rats, suggesting no effect of the PLA microsphere matrix on periodontal bone repair.

CONCLUSIONS

A long-term 25OHD delivery system is successfully prepared using an o/w emulsion–solvent evaporation technique. The formulation parameters could be adjusted to obtain microspheres with an average diameter of about 42 μm and an encapsulation efficiency of about 80%. Drug release from the prepared microspheres was almost steady during the experiment. These particles could protect BMSCs in a diabetic periodontitis-like environment and prevent alveolar bone loss in a rat model of diabetic periodontitis. This system may provide a potential approach in the treatment of this disease.

ACKNOWLEDGMENTS

REFERENCES

1. García-Hernández A, Arzate H, Gil-Chavarría I, Rojo R, Moreno-Fierros L. High glucose concentrations alter the biomineralization process in human osteoblastic cells. Bone. 2012;50:276–88.

2. O'Connell P, Taba M, Nomizo A, Foss Freitas M, Suaid F, Uyemura S, *et al.* Effects of periodontal therapy on glycemic control and inflammatory markers. J Periodontol. 2008;79:774–83.

3. Kim S, Kim K, Seo B, Koo K, Kim T, Seol Y, *et al.* Alveolar bone regeneration by transplantation of periodontal ligament stem cells and bone marrow stem cells in a canine peri-implant defect model: a pilot study. J Periodontol. 2009;80:1815–23.

4. Die L, Yan P, Jun Jiang Z, Min Hua T, Cai W, Xing L. Glycogen synthase kinase-3 beta inhibitor suppresses *Porphyromonas gingivalis* lipopolysaccharide-induced CD40 expression by inhibiting nuclear factor-kappa B activation in mouse osteoblasts. Mol Immunol. 2012;52:38–49.

5. Zhen D, Chen Y, Tang X. Metformin reverses the deleterious effects of high glucose on osteoblast function. J Diabetes Complications. 2010;24:334–44.

6. Gopalakrishnan V, Vignesh R, Arunakaran J, Aruldhas M, Srinivasan N. Effects of glucose and its modulation by insulin and estradiol on BMSC differentiation into osteoblastic lineages. Biochem Cell Biol. 2006;84:93–101.

7. Mealey B, Ocampo G. Diabetes mellitus and periodontal disease. Periodontology. 2007;44:127–53.

8. Venketaraman V, Lin A, Le A, Kachlany S, Connell N, Kaplan J. Both leukotoxin and poly-*N*-acetylglucosamine surface polysaccharide protect *Aggregatibacter actinomycetemcomitans* cells from macrophage killing. Microb Pathog. 2008;45:173–80.

9. Umeda J, Demuth DR, Ando E, Faveri M, Mayer M. Signaling transduction analysis in gingival epithelial cells after infection with *Aggregatibacter actinomycetemcomitans*. Mol Oral Microbiol. 2012; 27:23–33.

10. Dienelt A, Zur Nieden N. Hyperglycemia impairs skeletogenesis from embryonic stem cells by affecting osteoblast and osteoclast differentiation. Stem Cells Dev. 2011;20:465–74.

11. Bas A, Demirci S, Yazihan N, Uney K, Ermis KE. Nerium oleander distillate improves fat and glucose metabolism in high-fat diet-fed streptozotocin-induced diabetic rats. Int J Endocrinol. 2012;201(2):947187.

12. Sharma A, Bharti S, Kumar R, Krishnamurthy B, Bhatia J, Kumari S, *et al. Syzygium cumini* ameliorates insulin resistance and β-cell dysfunction via modulation of PPAR, dyslipidemia, oxidative stress, and TNF-α in type 2 diabetic rats. J Pharmacol Sci. 2012;3:205–13.

13. Watanabe K, Petro B, Shlimon A, Unterman T. Effect of periodontitis on insulin resistance and the onset of type 2 diabetes mellitus in Zucker diabetic fatty rats. J Periodontol. 2008;7:1208–16.

14. Pacios S, Kang J, Galicia J, Gluck K, Patel H, Ovaydi-Mandel A, *et al.* Diabetes aggravates periodontitis by limiting repair through enhanced inflammation. FASEB J. 2012;4:1423–30.

15. Hopfer U. Sorting out noncanonical, paracrine functions of vitamin D: focus on "Vitamin D receptor activation and downregulation of renin-angiotensin system attenuate morphine-induced T cell apoptosis". Am J Physiol Cell Physiol. 2012;303:C592–4.

16. Mercer K, Wynne R, Lazarenko O, Lumpkin C, Hogue W, Suva L, *et al.* Vitamin D supplementation protects against bone loss associated with chronic alcohol administration in female mice. J Pharmacol Exp Ther. 2012;343:401–12.

17. Zhou X, Han J, Song Y, Zhang J, Wang Z. Serum levels of 25-hydroxyvitamin D, oral health and chronic obstructive pulmonary disease. J Clin Periodontol. 2012;39:350–6.

18. Filippella M, Faggiano A, Falchetti A, Colao A, Rosa C, Poti C, *et al.* Risk of fractures and bone abnormalities in postmenopausal women with type 2 diabetes mellitus. Clin Cases Miner Bone Metab. 2010;7:126–9.

19. Geng S, Zhou S, Glowacki J. Effects of 25-hydroxyvitamin D(3) on proliferation and osteoblast differentiation of human marrow stromal cells require CYP27B1/1α-hydroxylase. J Bone Miner Res. 2011;26:1145–53.

20. Brownfield LA, Weltman R. Ridge preservation with or without an osteoinductive allograft: a clinical, radiographic, microcomputed tomography, and histologic study evaluating dimensional changes and new bone formation of the alveolar ridge. J Periodontol. 2012;83:581–9.

21. Chang P, Chung M, Wang Y, Chien L, Lim J, Liang K, *et al.* Patterns of diabetic periodontal wound repair: a study using micro-computed tomography and immunohistochemistry. J Periodontol. 2012;83:644–52.

22. Shive M, Anderson J. Biodegradation and biocompatibility of PLA and PLGA microspheres. Adv Drug Deliv Rev. 1997;28:5–24.

23. Kobayashi D, Tsubuku S, Yamanaka H, Asano M, Miyajima M, Yoshida M. *In vivo* characteristics of injectable poly(DL-lactic acid) microspheres for long-acting drug delivery. Drug Dev Ind Pharm. 1998;24:819–25.

24. Chung T, Huang Y, Liu Y. Effects of the rate of solvent evaporation on the characteristics of drug loaded PLLA and PDLLA microspheres. Int J Pharm. 2001;212:161–9.

25. Patomchaiviwat V, Paeratakul O, Kulvanich P. Formation of inhalable rifampicin-poly(L-lactide) microparticles by supercritical anti-solvent process. AAPS PharmSciTech. 2008;9:1119–29.

26. Park S, Jeon Y, Haam S, Park H, Kim W. Preparation of chitosan microspheres using membrane emulsification and its size modelling. J Microencapsul. 2004;21:539–52.

27. Quenelle D, Staas J, Winchester G, Barrow E, Barrow W. Efficacy of microencapsulated rifampin in *Mycobacterium tuberculosis*-infected mice. Antimicrob Agents Chemother. 1999;43:1144–51.

28. Barrow E, Winchester G, Staas J, Quenelle D, Barrow W. Use of microsphere technology for targeted delivery of rifampin to *Mycobacterium tuberculosis*-infected macrophages. Antimicrob Agents Chemother. 1998;42:2682–9.

29. Khaled K, Sarhan H, Ibrahim M, Ali A, Naguib Y. Prednisolone-loaded PLGA microspheres. *In vitro* characterization and *in vivo* application in adjuvant-induced arthritis in mice. AAPS PharmSciTech. 2010;11:859–69.

30. Kim K, Dean D, Wallace J, Breithaupt R, Mikos A, Fisher J. The influence of stereolithographic scaffold architecture and composition on osteogenic signal expression with rat bone marrow stromal cells. Biomaterials. 2011;32:3750–63.

31. Giacaman R, Asrani A, Ross K, Herzberg M. Cleavage of protease-activated receptors on an immortalized oral epithelial cell line by *Porphyromonas gingivalis* gingipains. Microbiology. 2009;155:3238–46.

32. Kang J, de Brito Bezerra B, Pacios S, Andriankaja O, Li Y, Tsiagbe V, *et al. Aggregatibacter actinomycetemcomitans* infection enhances apoptosis *in vivo* through a caspase-3-dependent mechanism in experimental periodontitis. Infect Immun. 2012;6:2247–56.

33. Xu H, Zhong H, Liu M, Xu C, Gao Y. Lappaconitine-loaded microspheres for parenteral sustained release: effects of formulation variables and *in vitro* characterization. Pharmazie. 2011;66:654–61.

34. Cui F, Cun D, Tao A, Yang M, Shi K, Zhao M, *et al.* Preparation and characterization of melittin-loaded poly(DL-lactic acid) or poly (DL-lactic-*co*-glycolic acid) microspheres made by the double emulsion method. J Control Release. 2005;107:310–9.

35. ElMeshad A, Tadros M. Transdermal delivery of an anti-cancer drug via w/o emulsions based on alkyl polyglycosides and lecithin: design, characterization, and *in vivo* evaluation of the possible irritation potential in rats. AAPS PharmSciTech. 2011;12:1–9.

36. Ford Versypt A, Pack D, Braatz R. Mathematical modeling of drug delivery from autocatalytically degradable PLGA microspheres—a review. J Control Release. 2013;165:29–37.

37. Chen X, Ooi C. Hydrolytic degradation and drug release properties of ganciclovir-loaded biodegradable microspheres. Acta Biomater. 2008;4:1046–56.

38. Li X, Deng X, Yuan M, Xiong C, Huang Z, Zhang Y, *et al. In vitro* degradation and release profiles of poly-DL-lactide–poly(ethyleneglycol) microspheres with entrapped proteins. J Appl Polym Sci. 2000;78:140–8.

39. Hosogi Y, Duncan M. Gene expression in *Porphyromonas gingivalis* after contact with human epithelial cells. Infect Immun. 2005;73:2327–35.

40. Yang L, Wang J, Fan Y, Chen S, Wang L, Ma J. Effect of 1,25(OH)(2)D(3) on rat peritoneal mesothelial cells treated with high glucose plus lipopolysaccharide. Cell Immunol. 2011;271:173–9.

41. Peng X, Vaishnav A, Murillo G, Alimirah F, Torres K, Mehta R. Protection against cellular stress by 25-hydroxyvitamin D3 in breast epithelial cells. J Cell Biochem. 2010;110:1324–33.

42. Zhang W, Zhao S, Li Y, Peng G, Han P. Acute blood glucose fluctuation induces myocardial apoptosis through oxidative stress and nuclear factor-κB activation. Cardiology. 2012;124:11–7.

43. Li H, Xie H, Fu M, Li W, Guo B, Ding Y, *et al.* 25-Hydroxyvitamin D(3) ameliorates periodontitis by modulating the expression of inflammation-associated factors in diabetic mice. Steroids. 2012;78:115–20.

44. von Hurst P, Stonehouse W, Coad J. Vitamin D supplementation reduces insulin resistance in South Asian women living in New Zealand who are insulin resistant and vitamin D deficient—a randomised, placebo-controlled trial. Br J Nutr. 2010;103:549–55.

45. Branco-de-Almeida L, Franco G, Castro M, Dos Santos J, Anbinder A, Cortelli S, *et al.* Fluoxetine inhibits inflammatory response and bone loss in a rat model of ligature-induced periodontitis. J Periodontol. 2012;83:664–71.

46. Yiu Y, Yiu K, Siu C, Chan Y, Li S, Wong L, *et al.* Randomized controlled trial of vitamin D supplement on endothelial function in patients with type 2 diabetes. Atherosclerosis. 2013;227:140–6.

47. Dörr J, Ohlraun S, Skarabis H, Paul F. Efficacy of vitamin D supplementation in multiple sclerosis (EVIDIMS Trial): study protocol for a randomized controlled trial. Trials. 2012;13:15.

48. Van der Velden U, Kuzmanova D, Chapple I. Micronutritional approaches to periodontal therapy. J Clin Periodontol. 2011;38(Suppl 11):142–58.

49. Garcia M, Hildebolt C, Miley D, Dixon D, Couture R, Spearie C, *et al.* One-year effects of vitamin D and calcium supplementation on chronic periodontitis. J Periodontol. 2011;82:25–32.